

An Precise Frequency Tracking Technique Based on Short Current Detection

Mahesh Thati & Mahesh Jonnala

¹Assistant Professor, Dept of EEE, Institute of Aeronautical Engineering college, Dundigal, Hyderabad.
E-mail: maheshthati216@gmail.com

²Masters in Power Electronic Systems from Osmania University, Hyderabad.
E-mail: mahesh.vikram023@gmail.com

ABSTRACT: *This paper suggests a short current control method to eradicate the short current by regulating the switching frequency to method the inherent frequency. When system running in force resonant mode, there will exist dangerous short current between the resonant network and the switching network when switching frequency drifts away from inherent frequency of the resonant network. Inductive Power Transfer (IPT) systems for transmitting tens to hundreds of watts have been reported for almost a decade. Most of the work has concentrated on the optimization of the link efficiency and have not taken into account the efficiency of the driver. A novel frequency tracking method based on short current detection is proposed for IPT applications. In addition, an instantaneous short current detection method utilizing cheap comparator is proposed. Furthermore, a fast and accurate tracking method is proposed to calculate the frequency mismatch and make a correction. The method can realize accurate frequency correction in several oscillation periods.*

KEYWORDS- Electromagnetic coupling, frequency control, inductive power transfer (IPT).

I. INTRODUCTION

Inductive power transfer (IPT) technology realizes efficient energy transfer across large air gap from power supply to electrical equipment. With its rapid development, more and more applications have been emerging in recent years such as mobile phone, electrical vehicle material handling, and biomedical implants. For a typical IPT system, resonant tanks are very commonly used to produce low-distortion sinusoidal oscillation and increase the system reactive capability. However, the inherent parameters of the resonant tanks may dynamically drift away from the designed parameters due to load variation and mutual coefficient change. It is because the

mutual coupling between the primary and secondary sides will produce dynamical reflection impedance in the primary resonant tank and cause its inherent frequency drifting. In order to realize soft switching, the topology switching signal must keep up with the inherent frequency variation. It should be noted here that the inherent frequency refers to the inherent soft switching frequency of the primary inverter, which transforms dc input to high-frequency ac output. Typical frequency tracking method is a passive tracking method, which completes topology switching by detecting the zero crossing points of resonant variables. This method is efficient to produce a self-sustained oscillation. However, it normally requires start-up control to produce initial oscillation, and the oscillation may fail in the low-quality-factor condition. Most important of all, this method cannot realize accurate frequency tracking. There inevitably exists a short-time lag in the topology switching due to the time delay and disturbance on gate driver and detection circuit in the feedback loop. The switching time lag will result in resonant waveform distortion and augment of switching loss. In particular, according to the first wireless power standard “Qi” the oscillation frequency in commercial IPT product should be set in the frequency range from 110 to 205 kHz. In the high-frequency range, the system becomes more complex and sensitive because many parasitic parameters will affect system performance. A tiny time delay or disturbance in the feedback path may cause the system performance to fall drastically. However, due to the inherently passive running property, it is impossible to eliminate the switching time lag and disturbance so that the frequency tracking error will always exist. Compared with the passive tracking method, an active tracking method which completes topology switching by external switching signal is seen to be a good alternate to solve these problems. However, it is greatly relied on

the tracking accuracy and speed. Since the inherent frequency is determined by an implicit high-order differential equation set, it is difficult to obtain its accurate value. Furthermore, even if the inherent frequency can be calculated, the time consuming will be unaffordable for real-time tracking. Therefore, instead of the complex calculation, a simple and real-time tracking method with unknown inherent frequency is needed. In the IPT system, it is well known that the short current is adverse which should be avoided. The short current occurs when resonant tank is shorted by the switching network. It is caused by mismatch between the driving frequency and the inherent soft switching frequency of the resonant tank. A large mismatch can produce dangerous high current which may cause the switching devices to fail. It has been found that the short current occurs almost instantaneously while the mismatch appears. Therefore, it can be utilized as a fast and accurate ruler to measure the frequency error.

A basic IPT systems architecture consists of several modules, as illustrated in Fig. 1. The architecture includes dc power supply units (PSUs), coil driver (i.e. clock generator and power amplifier (PA) having an impedance matching network), transmitting (TX) coil with separation distance D from a receiving (RX) coil (measured from the centre-to-centre of the coils), an optional rectifier/regulator and a load. To fully characterize the complete system, the end-to-end efficiency η_{ee} of all the building blocks, from the ac source to the load, can be considered as follows; where the efficiency terms are shown on Fig. 1

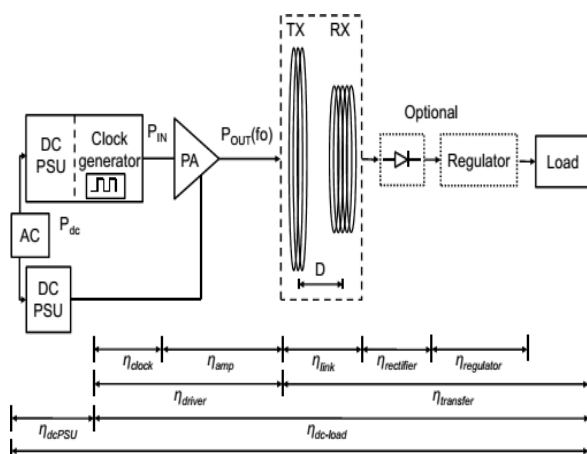
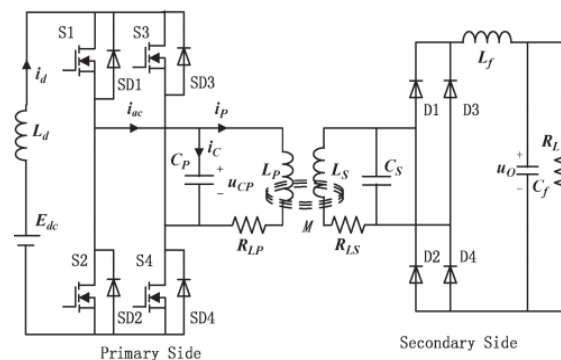


Fig. 1. Inductive power transfer systems architecture

For a typical IPT system, resonant tanks are very commonly used to produce low-distortion sinusoidal oscillation and increase the system reactive capability. However, the inherent parameters of the resonant tanks may dynamically drift away from the designed parameters due to load variation and mutual coefficient change [10], [11]. It is because the mutual coupling between the primary and secondary sides will produce dynamical reflection impedance in the primary resonant tank and cause its inherent frequency drifting. In order to realize soft switching, the topology switching signal must keep up with the inherent frequency variation. It should be noted here that the inherent frequency refers to the inherent soft switching frequency of the primary inverter, which transforms dc input to high-frequency ac output. Typical frequency tracking method is a passive tracking method, which completes topology switching by detecting the zero crossing points of resonant variables [12]–[15]. This method is efficient to produce a self-sustained oscillation.

II. THEORY AND METHODOLOGY

In terms of structures of resonant network at primary side, there are normally two types. One is parallel resonant, and the other is series resonant. The short current typically appears in parallel resonant structure. A typical parallel-resonant-type ICPT system is shown in Fig. 2



As can be shown, the inductively coupled power transfer (ICPT) system can be divided by primary and secondary sides.

- 1) At the primary side, the dc input E_{dc} and filter compose a quasicurrent source.
- 2) In addition, the switching network consists of two switch pairs (S1, S4) and (S2, S3) and their inherent inverse parallel diodes (SD1–SD4).
- 3) The two switch pairs operate complementarily at the forced switching frequency, transform dc current input to high-frequency square-wave current, and
- 4) Inject it into the resonant network, which is composed of resonant inductor L_p , capacitor C_p , and equivalent series resistance (ESR) resistance R_{LP} .

The resonant network converts the square-wave current to sinusoidal current for primary coil to produce alternating magnetic field.

- 1) At the secondary side, the secondary coil will pick up energy from the magnetic field and produce resonance in the parallel resonant network composed of resonant inductor L_s and capacitor C_s .
- 2) With the rectifier and filter network (L_f, C_f), ac energy is transformed to dc output to the load (R_L).
- 3) While the forced switching frequency is approaching the inherent soft switching frequency of the primary resonant network, the switching points will be close to the zero crossing points of the resonant voltage u_{CP} which can produce zero-voltage-switching conditions.

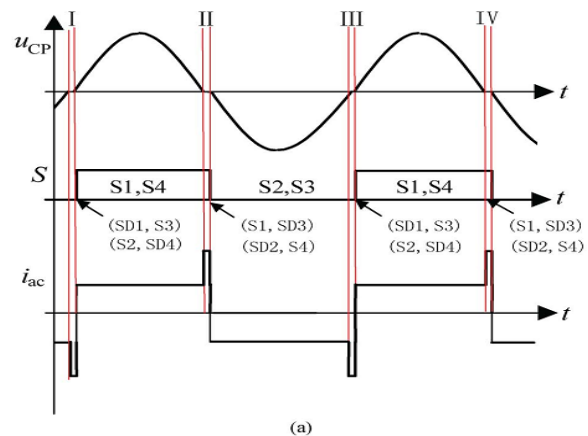
In system running, when the switching frequency drifts away from the inherent frequency, there are two possible cases. One is higher, and the other is lower than the inherent frequency. The two cases are quite different in nature and should be analyzed, respectively.

A. Higher Case

As it can be seen from (a), the waveforms from up to down are resonant capacitor voltage u_{CP} , switching signal S , and the input current i_{ac} of the resonant tank, respectively. For the switching frequency is higher than the inherent frequency, the switching instants will appear before the zero switching points of u_{CP} . In addition, the mismatches will produce four short current regions

(Region I–IV). In each region, the short current has different path and can be illustrated from (b) to (e), respectively.

- a) In Regions I and III, the switch pair (S1, S4) turns on and the switch pair (S2, S3) turns off. However, as the resonant voltage u_{CP} is below zero, two short current loops will form in the inverter bridge.
- b) The one shown in (b) is the upper short current loop including S1 and SD3.
- c) The other shown in (d) is the lower loop include SD2 and S4.
- d) In Regions II and IV, the switch pair (S1, S4) turn on and (S2, S3) turn off. However, the resonant voltage u_{CP} is above zero.
- e) Similarly, there are two short current loops. The one shown in (c) is the upper one including SD1 and S3, and the other shown in (e) is the lower one including S2 and SD4.
- f) As the total resistance in the short current path is approaching zero, the short current can be very large and result in the sharp peak of input current i_{ac} shown in (a).



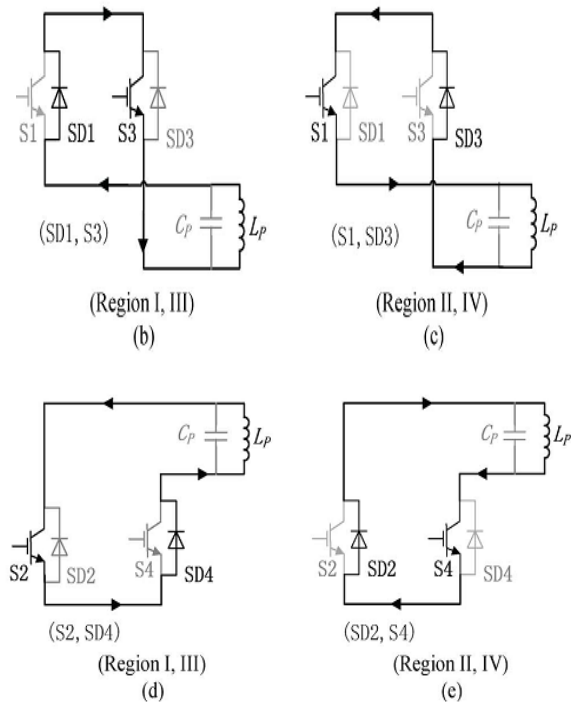


Fig. 3. Switching frequency lower case. (a) Operating waveforms when short current occurs. (b) (Regions I and III) Upper short current loop. (c) (Regions II and IV) Upper short current loop. (d) (Regions I and III) Lower short current loop. (e) (Regions II and IV) Lower short current loop.

B. Lower Case

When the switching frequency is lower than inherent frequency, the short current will appear as well. However, it is different from the higher case in nature. The lower case can be illustrated in Fig. 3. As it can be seen from (a), since the switching frequency is lower than the inherent frequency, the switching instants will lag behind the zero crossing points of u_{CP} .

- Furthermore, the mismatches will produce four short current regions (Regions I–IV).
- In Regions I and III, when the resonant voltage u_{CP} crossing the zero, the switching pair (S2, S3) still maintains ON STATE because the switching signal is lagged behind.
- Two short current loops will form in the upper and lower bridges, respectively. The one

- including SD1 and S3 is shown in (b), and the other including S2 and SD4 is shown in (d).
- In Regions II and IV, the switch pair (S1, S4) will maintain ON STATE. Similarly, the upper short current loop including S1 and SD3 is shown in (c), and the lower one including SD2 and S4 is shown in (e).
- However, it should be noted that the short current is driven by resonant inductor L_p instead of capacitor C_p as the resonant voltage is clamped to zero.
- Therefore, the short current peak of input current i_{ac} shown in (a) is much lower than that of the higher case.
- In addition, in higher case, the short current appears at the front end of the switching signal, while in the lower case, it appears at the back end.

III. SHORT CURRENT ANALYSIS

Since the principles of the short current are quite different in the higher and lower cases, the short current analysis should be given, respectively.

A. Higher Case

According to the analysis of the Section III, the equivalent circuit of the short current loop can be shown in Fig. 4.

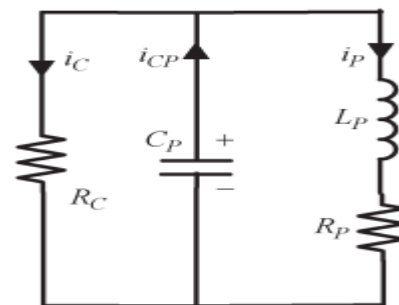


Fig. 4. Equivalent circuit of short current loop.

As can be seen, the short current is i_C , and resistance R_C is the sum of conducting resistances of switch devices and diodes on the short current loop. Moreover, the resistance R_p is the sum of E_{SR} resistance R_{LP} and reflecting resistance from secondary side.

B. Lower Case

In the lower case, the resonant voltage is clamped to zero and cannot drive the short current. The short current is actually the freewheeling current of the resonant inductor L_p .

The equivalent circuit of the short current loop can be shown in Fig. 5. In the short-time interval of the short current, the resonant current i_p can be seen as a constant, which equals the instant detection circuit current $i_p(0)$ when the short current occurs.

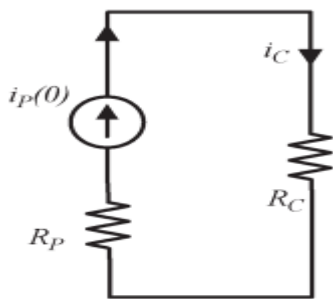


Fig. 5. Equivalent circuit of short current loop.

IV. FREQUENCY TRACKING CONTROLS

The frequency tracking control is to make the switching frequency accurately and rapidly keep up with the inherent frequency variation of the resonant tank.

A. Short Current Detection

However, as the duration time of the short current is normally less than $1 \mu s$, it is quite difficult for normal analog to digital chip to detect it. In this paper, a short current detection circuit using normal comparator chip LM319 is designed. It can be shown in Fig. 6.

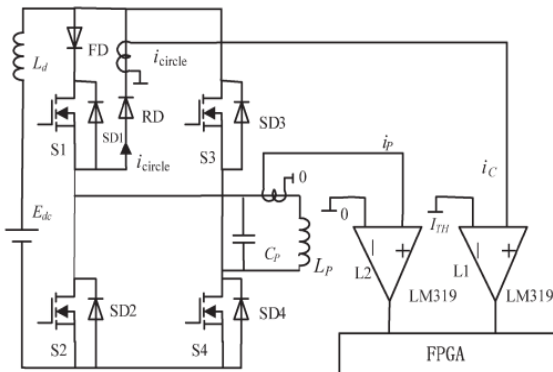


Fig. 6. Short current detection circuit.

As can be seen, a comparator L1 is used to detect the duration time T_C of the short current. As analyzed in Section III, two identical short currents will form in the upper and lower bridges simultaneously in no matter the higher or the lower case. Moreover, in the upper bridge, the two short current loops should include (SD1, S3) and (S1, SD3) in no matter the higher or the lower case.

It can be seen that the short current in any diode of SD1–SD4 will be identical. In order to simplify the detection circuit, only SD1 is selected to detect the short current. However, as the inherent diode SD1 is normally embedded in switch device, it is difficult to detect the current on it. Therefore, an inverse parallel diode recovery diode (RD) with low conduction resistance is added to replace it. In addition, a block diode is put in series with the switch S1 to invalidate the diode SD1. Furthermore, with a current transformer, the short current on RD can be detected.

B. Determining the Mismatch Direction

The second step of tracking is to determine whether the frequency is higher or lower than the inherent frequency. As can be seen from Figs. 2 and 3, the short current on SD1 will select different occurrence regions for the higher or lower case. For higher case, the short current will select Regions II and IV for occurrence, and for the lower case, the short current will select Regions I and III.

C. Mismatching Calculation and Correction

The third step of tracking is to calculate the deviation between the switching frequency and the inherent frequency.

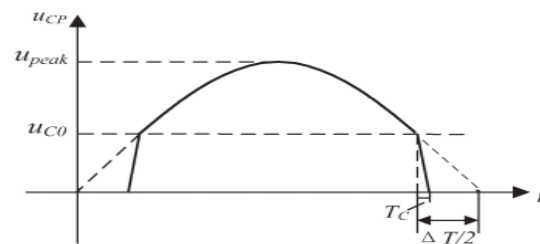


Fig. 7. Frequency mismatch calculation method for the higher case.

The tracking method should be different according to the higher and lower cases. For the higher case, the frequency mismatching calculation method can be illustrated in Fig. 7.

V. SIMULATION RESULTS

A practical investigational IPT system has been built to verify the proposed tracking method which exploits an FPGA chip as the tracking controller. The experimental system structure.

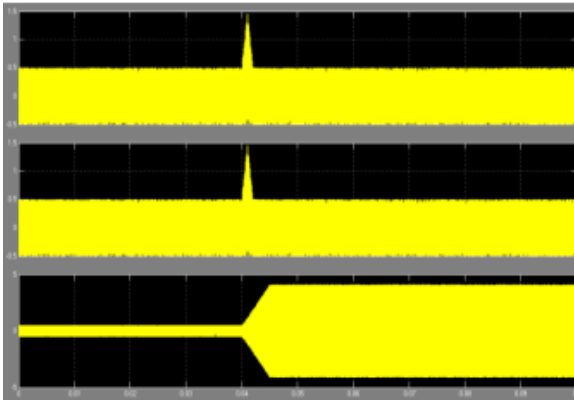


Fig. 8. Waveforms of the system start process

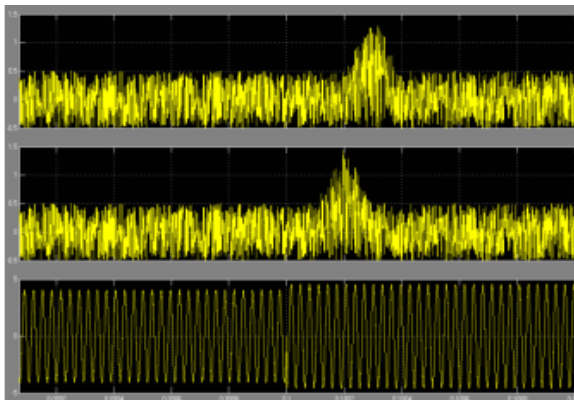


Fig. 9. Waveforms of load change from R2 to R1 (from light to heavy load conditions).

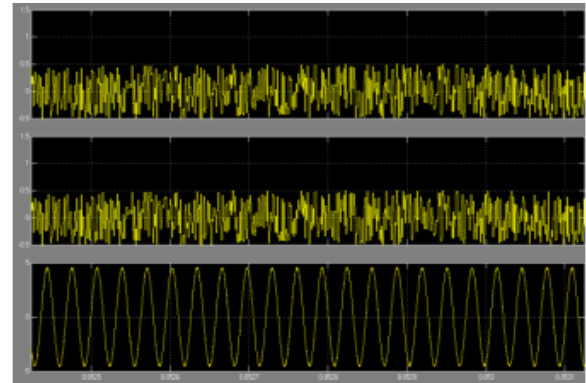


Fig. 10. Waveforms of load change from R1 to R2 (from heavy to light load conditions)

VI. CONCLUSION

In this paper, a new accurate frequency tracking method based on short current detection has been proposed for an IPT system. An instantaneous short current detection method utilizing cheap comparator is proposed. Furthermore, a fast and accurate method is proposed to calculate the frequency mismatch and make a correction. Compared with the conventional autonomous oscillation method, this method is an active one which can overcome the common problems such as feedback delay, resonant failure, and additional start-up circuit.

REFERENCES

- [1] M. Budhia, V. Vyatkin, and G. A. Covic, "Powering flexible manufacturing systems with intelligent contactless power transfer," in 6th IEEE International Conference on Industrial Informatics, pp. 1160-1165, 2008.
- [2] S. Y. R. Hui and W. W. C. Ho, "A new generation of universal contactless Battery Charging platform for portable Consumer Electronic equipment," IEEE Trans. on Power Electron., Vol. 20, pp. 620-627, 2005.
- [3] J. A. A. Qahouq, O. Abdel-Rahman, L. Huang, and I. Batarseh, "On load adaptive control of voltage regulators for power managed loads: Control schemes to improve converter efficiency and performance," IEEE Trans. on Power Electron., Vol. 22, No. 5, pp. 1806-1819, Sep. 2007.

[4] Y. Wu, L. Yan, and S. Xu, "A new contactless power delivery system," in 6th International Conference on Electrical Machines and Systems, pp.253-256, 2003.

[5] L. Zhao, C. F. Foo, K. J. Tseng, and W. K. Chan, "Transcutaneous transformers in power supply system for an artificial heart," in International Conference on Power Electronic Drives and Energy Systems for Industrial Growth, pp. 348-352, 1998.

[10] J. U. W. Hsu, A. P. Hu, and A. Swain, "Fuzzy logic-based directional fullrange tuning control of wireless power pickups," IET Power Electron., vol. 5, no. 6, pp. 773-781, Jul. 2012.

[11] J. U. W. Hsu, A. P. Hu, and A. Swain, "A wireless power pickup based on directional tuning control of magnetic amplifier," IEEE Trans. Ind. Electron., vol. 56, no. 7, pp. 2771-2781, Jul. 2009.

[12] B. Sharp and H. Wu, "Asymmetrical voltage-cancellation control for LCL resonant converters in inductive power transfer systems," in Proc. IEEE Appl. Power Electron. Conf. Expo., Orlando, FL, USA, Feb. 5-9, 2012, pp. 661-666.

[13] W. Yanzhen, A. P. Hu, D. Budgett, S. C. Malpas, and T. Dissanayake, "Efficient power-transfer capability analysis of the TET system using the equivalent small parameter method," IEEE Trans. Biomed. Circuits Syst., vol. 5, no. 3, pp. 272-282, Jun. 2011.

[14] T. D. Dissanayake, A. P. Hu, S. Malpas, L. Bennet, A. Taberner, L. Booth, and D. Budgett, "Experimental study of a TET system for implantable biomedical devices," IEEE Trans. Biomed. Circuits Syst., vol. 3, no. 6, pp. 370-378, Dec. 2009.

[15] S. Ping, A. P. Hu, S. Malpas, and D. Budgett, "A frequency control method for regulating wireless power to implantable devices," IEEE Trans. Biomed. Circuits Syst., vol. 2, no. 1, pp. 22-29, Mar. 2008

BIODATA



Mahesh Thati, a teaching experience of 6 years i.e. from 2012 to 2017 and currently Working as Assistant Professor in Institute of Aeronautical Engineering college, Dundigal, Hyderabad.



Mahesh Jonnala completed Masters in Power Electronic Systems from Osmania University, Hyderabad.